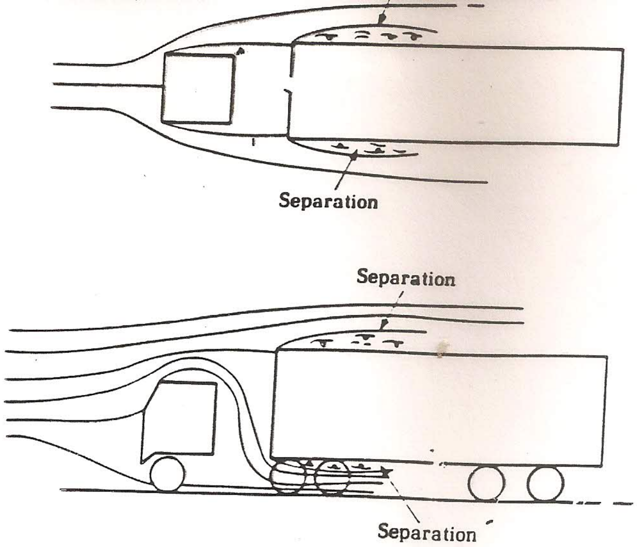

FIGURE 6.22
Plan and profile views of streamlines about a cab-over-engine tractor-trailer combination.

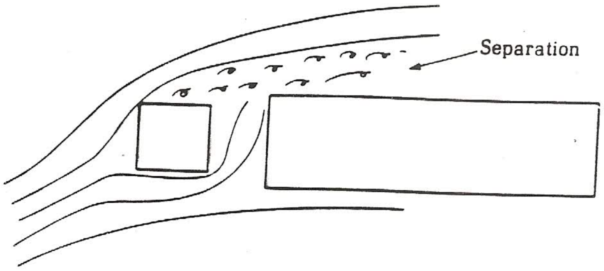

FIGURE 6.23
Plan view of the flow pattern on a yawed truck.

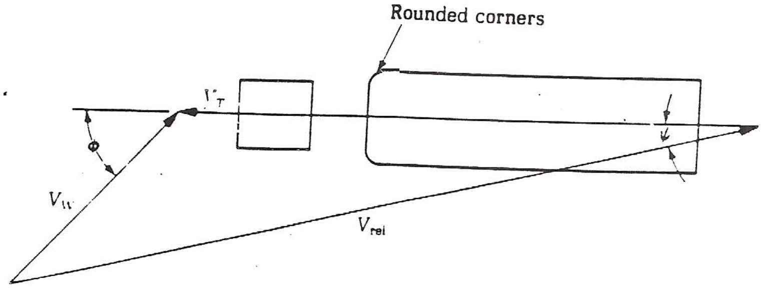

FIGURE 6.24
Wind velocity diagram for analysis of flow about a truck.

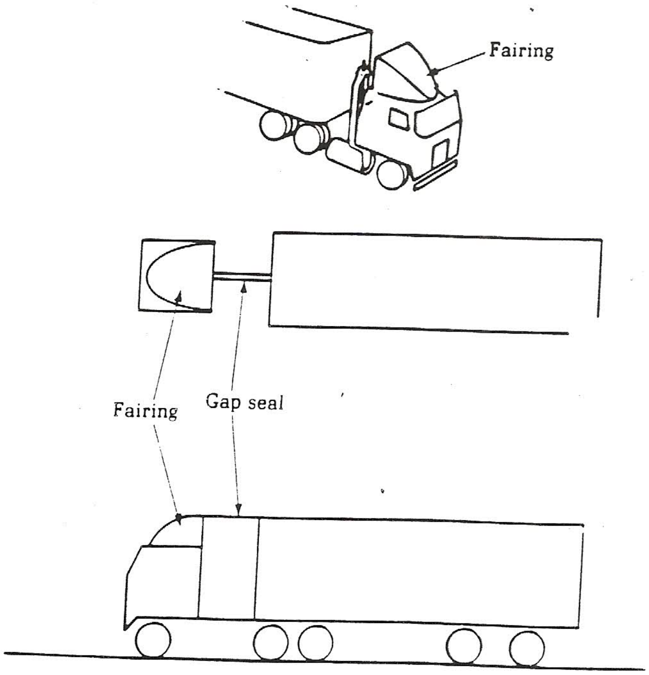

FIGURE 6.25
A fairing and gap seal attached to a tractor-trailer truck.

Ground Effect. In wind-tunnel investigations and in full-scale calculations there does not seem to be any established rule to account for variation and distribution of speed with altitude, as far as wind loads on buildings and structures are concerned. On the floor of the tunnel or on a ground board, a boundary layer is usually present that is lower than the obstacle investigated. Drag coefficients are then referred to the undisturbed dynamic pressure above the layer. Pressures are given in form of the non-dimensional coefficient

$$C_p = (p_{local} - p_{ambi})/(0.5\ \varrho\ V^2) \qquad (2)$$

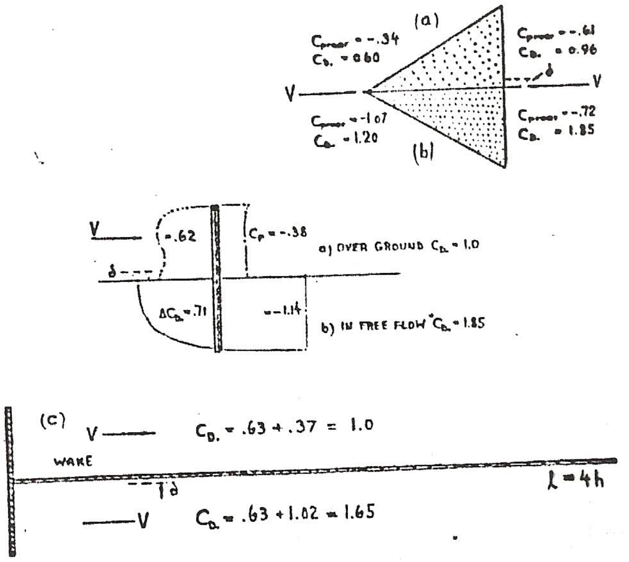

Figure 2. Pressure and drag coefficients of bluff shapes, tested between tunnel walls (3,a):
a) half bodies mounted over floor of tunnel,
b) in free flow (complete double models),
c) demonstrating influence of "splitter" plate.

Figure 2 shows that the b'layer has a considerable influence upon pressure distribution and drag of simple bluff obstacles. The experiment in part (c) of the illustration demonstrates the influence of the ground on the vortex street developing behind two-dimensional obstacles (see in the "pressure drag" chapter). With the board ("splitter" plate) ahead of the two-dimensional plate, face- and rear-side pressures are somewhat reduced as against conditions in free flow. With the board behind the plate, the vortex street is evidently suppressed; the value of the rear-side pressure is considerably reduced from $C_p = -1.14$ to -0.37, and the drag coefficient is only ≈ half of that in free flow. In a three-dimensional plate (*figure* 3), the drag coefficient is not affected, however, by the presence of the ground. On the other hand, because of interference with its flow pattern, the drag coefficient of the streamline body in figure 3.b (with b'layer-sensitive flow separation from the rear), is ≈ doubled. Since buildings are usually of bluff and three-dimensional shape, the

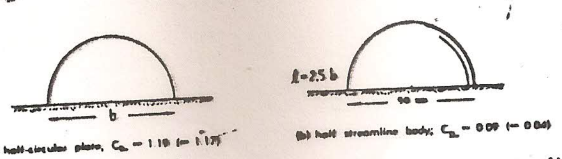

Figure 3. Drag coefficients of two three-dimensional bodies (seen in direction of flow) mounted over a ground surface (3,b), tested at $R_b = 2\ 10^5$ where b = 90 mm. The values in brackets indicate drag coefficients in free flow (on double models).

type of their flow pattern does not appear to be affected by the atmospheric boundary layer. The magnitude of their drag coefficients corresponds to the mechanism of protuberances as explained in the chapters on "irregularities" and "interference"; in other words, their drag approximately corresponds to the average dynamic pressure within their height.

2. VARIOUS BUILDINGS

Houses. Figure 4 presents the pressure distribution of a house. There is positive pressure on flat surfaces facing the wind. In the separated space behind the house, the pressure is uniform and negative, between $C_p = -0.2$ and -0.8 (depending on building shape and wind direction). In sharp-cornered buildings, the flow may also be separated from the lateral walls. References (4,b and c) show that the flow can also be separated from the windward side of roofs as illustrated in figure 4 - particularly with slopes smaller than 45° and in taller buildings (with h/l exceeding unity. Figure 5, on the other hand, is an example where the flow reattaches to the windward side of the roof. This illustration also demonstrates that the distribution is little or not at all affected by the particular shape of the rear side. Wind directions different from the one in the two illustrations are investigated in (4). Reference (4,c) also gives information on the mutual interaction between several houses placed one behind the other in a row.

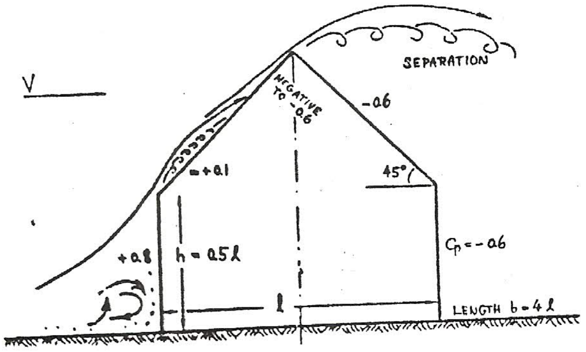

Figure 4. Flow pattern and pressure distribution (on center line) of a simple house shape (4,b).

as the sphere. In this respect is tentatively:

$$\frac{R_{crit}}{R_{crito}} = \sqrt{\frac{V^2}{V^2 + (k \cdot u)^2}} = \frac{1}{\sqrt{1 + (k \cdot u/V)^2}}$$

where k < 1 represents a suitable integration constant. This effect is demonstrated in figure 24 at (t); the critical Reynolds number of the sphere as tested is shifted from R_{dcrit} = 2.9 10^5 (without rotation) to 2 10^5 as shown in the graph at u/V ≈ 1.8; hence k ≈ 0.6. The sphere also exhibits the centrifugal effect at "c". Note that the low sphere value $C_{D\bullet}$ = 0.38 in subcritical condition (instead of ≈ 0.47) is caused by type and size of the support in these tests by means of a rotating shaft.

The Human Body is similar in aerodynamic shape to a cylinder with a length ratio h/"d" between 4 and 7. Since human beings vary very much in size and proportions, selection of a reference area is difficult. Figure 25, therefore, presents the drag of an average man in the form of drag area D/q. The drag is predominantly a function of the projected frontal area in the various positions tested. Based on estimated areas, drag coefficients can be determined for the standing positions between $C_{D\bullet}$ = 1.0 and 1.3. Without clothing, the drag is between 5 and 10% less than listed.

How Fast a Man Falls. After bailing out of an airplane, and before releasing the parachute, the body of a man accelerates to a terminal velocity the magnitude of which can be derived from W = D = q (D/q). Near sea level (where ρ = 0.0024 lb sec²/ft⁴), the falling speed of a man with W = 180 lb, is accordingly $V_{ft/sec} \approx 400 \sqrt{(D/q)}$. Employing the drag areas as listed in figure 25 (between 1.2 and 9.0 ft²), speeds between 130 and 370 ft/sec are thus obtained. Terminal velocities are reported (32,c) between 150 and 180 ft/sec "near sea level"; without specification as to position and attitude during free fall. Another source (32,c) gives a drag area of 5 ft² for a "rolling and somersaulting" man. To give a certain scale to all these numbers, it is mentioned that the drag area of a typical fighter airplane is in the order of 6 ft².

The Drag of Ski-Runners has been tested in wind tunnels. In upright position (going down a slope) a drag area D/q = 5.5 ft² is found (32,a) in a smooth wooden model. A similar value (≈ 6.5 ft²) can be derived from (32,b) on the basis of an estimated frontal area in the order of 7 ft². Both sources also give results on drag and lift of a ski-jumping man. In the typical "flying" position, with the body leaning forward against and onto the air, the lift area (including the contribution of the skis) is in the order of L/q = 2.5 ft²; the maximum lift/drag ratio is in the order of "1".

6. DRAG OF VARIOUS TYPES OF PLATES

All that is said in the preceding section about the critical effect of the boundary layer upon the drag of spheres, applies in principle to all sufficiently rounded bodies, such as the strut sections for instance in Chapter VI. On the other hand, bodies with sharp edges, such as disks and plates in a flow normal to their surfaces, do not show any critical drag decrease. The pressure gradient around the sharp edges would necessarily be extremely high for a flow pattern attached to the rear of a plate — that is, theoretically from Δp/q = −∞ at the edge to + 1 at the rear stagnation point. No boundary layer, whether laminar or turbulent, can follow the way around the edges of such plates.

Small R'Numbers. Figure 26 shows the drag coefficient of disks and square plates in normal flow, as a function of Reynolds number. Below R_d = 100, there is the regime of predominantly viscous flow as discussed in the beginning of this chapter. Approximately at R_d = 300, the drag coefficient of the disk shows a peak, as reported from two independent sources. Observation of the flow pattern (35) proves this peak to be due to a change in the pattern of the vortex system behind the body.

Turbulence Effect. Above R_d = 1000, the drag coefficient of disks (and other plates) is practically constant up to the highest Reynolds numbers ever tested (approaching 10^7). Because of this stability,

Figure 25. Drag areas (D/q in ft²) of an average man in various positions, tested in a wind tunnel (31) at speeds between 100 and 200 ft/sec. Specifications: W = 165 lb; h = 5.9 ft; ∇ = 2.6 ft³; S_{wet} = 20 ft².

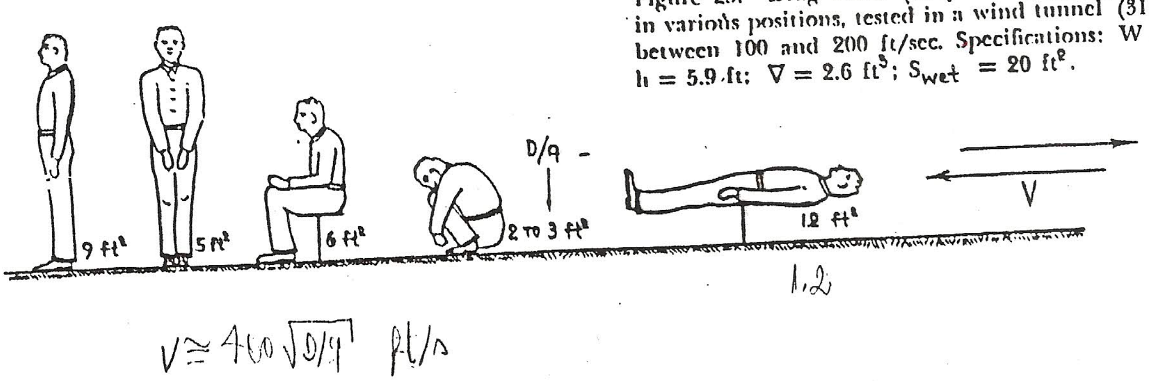

V ≅ 400 √(D/q) ft/s

33